International Journal of Engineering Trends and Technology
ISSN: 2231–5381 / https://doi.org/10.14445/22315381/IJETT-V72I12P127

Volume 72 Issue 12, 320-329, December 2024

Original Article

Study of Harmful Algal Blooms in Lake Titicaca from 2018 to 2023 based on Landsat 8 Satellite

Natalia I. Vargas-Cuentas[1], Elber E. Canto-Vivanco[2], Sebastian Ramos-Cosi[3], Avid Roman-Gonzalez[4]

[1,2,3,4]*Image Processing Research Laboratory (INTI-Lab), Universidad de Ciencias y Humanidades, Lima, Peru.*

[1]*Corresponding Author : nvargas@uch.edu.pe*

Received: 30 May 2024 Revised: 07 October 2024 Accepted: 10 October 2024 Published: 25 December 2024

Abstract - *Inorganic substances such as nitrogen and phosphorus increase the proliferation of algae in water bodies. Besides, human-generated waste enhances the effects of eutrophication. Given this problem, the present study has the primary objective of performing an analysis of harmful algal blooms in Lake Titicaca using remote sensing images from Landsat 8 satellites to calculate the Normalized Difference Vegetation Index (NDVI), Green Chlorophyll Index (CI-Green), Surface Algal Bloom Index (SABI), and Chlorophyll Vegetation Index (CVI). Our results indicate that the highest averages of the four indices correspond to 2022, followed by 2020. The present study reveals that areas with concentrations of vegetation (algae) and chlorophyll activity are in Huancané, Puno, El Collao, and Chucuito (Peru), while in Bolivia, they are in the provinces of Omasuyos, Los Andes, and Ingavi.*

Keywords - *Remote sensing, Landsat 8, NDVI, CI-Green, SABI-CVI.*

1. Introduction

Eutrophication is the process by which inorganic substances, such as nitrogen and phosphorus, accumulate in a body of water with slow flow, often surrounded by land, leading to the rapid growth of algae and plankton [1]. Although eutrophication occurs naturally, human-generated waste significantly amplifies its impact [2]. According to UN-Water reports, 40% of monitored water bodies fail to maintain acceptable environmental quality [3]. Pollution in aquatic environments fosters conditions that promote Harmful Algal Blooms (HABs), representing the excessive growth of algae populations that can severely disrupt marine ecosystems. These blooms threaten wildlife, natural resources, and human health by degrading water quality and altering marine life balance [4]. For instance, data from the Florida Department of Environmental Protection (DEP) reveals that 70% of Lake Okeechobee's surface is affected by HABs [5]. Similarly, the European Union reports that HABs in the Oder River led to the death of 360 tons of fish [6]. Regarding Peru, in [7], it was revealed that the death of 75% of Myloplus Schomburgkii fish in an Amazonian pond was due to the presence of Lemna minor. On the other hand, in [8], high concentrations (>2.11x105 cel.L-1) of the microalga Blixaea quinquecornis were recorded on the coasts of Miraflores and Paracas, causing the mortality of fish and mollusks. A similar situation occurs in Lake Titicaca, a body of water spanning 8562 km² between Peru and Bolivia at an altitude of 3809 meters above sea level [9]. In [10], it was determined that from 2016 to 2018, turbidity in the Katari River basin in Bolivia increased by 155% due to urban population growth, industrial development, and agricultural and mining activities. On the Peruvian side, [11] identified antibiotic residues (>78.2 ng. L^{-1}) in the Chimu drinking water supply, attributed to aquaculture activities and wastewater discharge. This increasing pollution has led to the proliferation of Harmful Algal Blooms (HABs). Over the past two decades, the rapid growth of photosynthetic microorganisms such as *Lemna sp.*, *Microcystis aeruginosa*, and *Carteria sp.* have been reported. Moreover, data from the Permanent Observatory of Lake Titicaca (OLT) show that chlorophyll-a concentrations in 2021 reached levels 5 to 9 times higher (up to 28 µg. L^{-1}) than in 1980 (3 µg. L^{-1}), indicating a significant presence of algae and cyanobacteria [12]. The present study uses remote sensors to analyze harmful algal bloom proliferation in Lake Titicaca. For this purpose, satellite images from the Landsat 8 mission are used to extract parameters such as the Normalized Difference Vegetation Index (NDVI), Green Chlorophyll Index (CI-Green), Surface Algal Bloom Index (SABI), and Chlorophyll Vegetation Index (CVI). These parameters are used to identify areas of the lake with the presence of algal blooms. In order to calculate the four mentioned indices, the spectral bands used were red, green, blue, and near-infrared. Therefore, this research aims to analyze harmful algal blooms in Lake Titicaca using remote-sensing images from Landsat 8. The analysis will cover the period from 2018 to 2023 to examine the temporal patterns of Harmful Algal Blooms (HABs). Satellite imagery with less than 10% cloud cover will be selected for these five years. The images will undergo

preprocessing steps, including radiometric and atmospheric calibration. Subsequently, four indices will be calculated for each image, with the annual average of each parameter determined for every year analyzed. Finally, maps highlighting the results will be produced, pinpointing the areas within Lake Titicaca affected by algal blooms. These maps will provide valuable insights for decision-makers in Peru and Bolivia, who jointly manage this vital water resource, allowing them to implement proactive and informed management strategies.

2. Revision of the Literature

Satellite remote sensing uses remote sensors that provide the opportunity to obtain information about an object from a distance, which is helpful for various types of studies, including detecting algal blooms with the assistance of satellite missions [13], [14]. Over the years, many satellite missions have been deployed to take photographs of the Earth's surface; they are widely used in various studies due to easy access to the products from the satellites. These satellite missions can be Moderate Resolution Imaging Spectroradiometer (MODIS), Sentinel-3 with its Ocean and Land Colour Instrument (OLCI), Landsat 8 with its Operational Land Imager (OLI) or previous Landsat missions, the Advanced Very High Resolution Radiometer (AVHRR) of the National Oceanic and Atmospheric Administration (NOAA), among others.

In [5], images provided by NOAA were used to evaluate the blue-green algal bloom potential in Lake Okeechobee, located in Florida, USA. Based on that, the Florida Department of Environmental Protection collected samples in 55 points and found that 38 had algal bloom conditions. In [10], images from Landsat 7 mission were used to study the land cover and land use of theKatari River Basin located in Bolivia, where urban population growth and economic activities like agriculture, mining and industries have profound impact on the water quality of the Titicaca Lake, this image served for generate land cover maps from 2006 to 2018, differentiating six classes: water, built up, vegetation, barren land, shrubs/grass, and snow cover through indexes calculation.

Meanwhile, in [13], HABs were identified in Chesapeake Bay, USA, using OLCI images. It is crucial to evaluate the coverage of HABs in water bodies, and this can be achieved using indices to represent the condition of the surface of the water bodies and show through a color palette the severity of HAB and the most affected areas due to human activities. Considering that eutrophication, intensified by human activities, drives the growth of algae and weeds, thus affecting the ecosystem balance, a monitoring study was conducted in [2] using satellite imagery in Lake Maracaibo, Venezuela. The Aqua/MODIS captured the images. NDVI values were obtained using reflectances in the red and near-infrared channels, resulting in a range from -1 to 1, with values greater than 0.1 indicating the presence of water lentils (Lemnaceae family). As a result, it was found that for 2003-2006, the areas covered by this alga represented 0.01%, 11%, 1.5%, and 7%, respectively. Furthermore, in [15], a model was sought to estimate chlorophyll-a concentrations in the Vaal Dam, South Africa, to identify Anabaena and Microcystis species using Landsat 8 OLI imagery. Field data collection was also conducted to validate the prediction model. The model revealed that the red band (0.66 µm) negatively correlated with chlorophyll-a density.

In comparison, the near-infrared band (0.68 µm) had a positive correlation, thus validating the utility of both indices and individual spectral bands for estimating chlorophyll-a concentration in the turbid waters of Vaal Dam. The same satellite mission was used in [16] for monitoring algal blooms due to concentrations of microorganisms such as Microcystis sp., Ceratium sp., Oscillatoria sp., Cyclotella sp., Aulacoseria sp., and Clostertopsis sp. in the San Roque Reservoir, Argentina. Samples were collected at 8 points in the reservoir, and Landsat 8 OLI imagery was used.

Additionally, chlorophyll-a and trophic state index maps were generated. Field sample results showed that four of the studied points had high chlorophyll-a concentrations, with the two highest (288.5 and 197.1 µg/L) exhibiting high reflectance in the green band (565 nm). On the other hand, in [9], it is mentioned that remote sensing requires sensors with adequate spatial resolution, spectra, and radiometry. Therefore, a simulation was performed in HydroLight for oligotrophic lakes based on Lake Titicaca to obtain reflectivities of different chlorophyll-a types. Convolutions were then performed with the spectral responses of Landsat 8 and subsequently with MODIS to validate the former. OC2 and OC3 algorithms were calibrated for Landsat 8, and when calibrated with NOMAD, a low correlation of 0.67 was obtained, while calibration with HydroLight resulted in a high correlation of 0.84.

Obtaining the data is just one of the first steps in remote sensing; because an image taken by a satellite could be composed of several band reflectances, it is necessary to calculate indices. How reflectances interact varies depending on the index formula applied. Thus, knowing what characteristic of a phenomenon or place is intended to be studied is indispensable. In the state-of-the-art, many indices identify features such as vegetation cover, cloudiness, and water bodies. Even in a single theme, like vegetation, variants can be found for more specific characteristics, e.g., canopy, algal blooms, and chlorophyll activity. In [14], it was used every single band from Landsat 8 OLI and a simple ratio to identify suspended solids on a Korean river, finding that the NIR band and the simple ratio NIR/blue are sensitive to suspended solids, showing that working with single bands is not as effective, and better results can be achieved using ratios or indices. The most widely used index for detecting

vegetation cover is the Normalized Difference Vegetation Index (NDVI), used in [2] because that index can differentiate vegetation from other things and even differentiate vegetation health levels. Some studies use more than one index to obtain a more accurate or complete result, such as in [10], where three indices were used to determine the eutrophication level in a water body.

However, existing indices are not always used; some works propose new indices or a modification that can adapt to their object of study; some of those contributions can even be useful for other studies, as well as in [9], where two algorithms were modified to match the results of remote sensing and in situ sample collection.

3. Materials and Methods

3.1. Study Area Description

Lake Titicaca is considered the world's highest navigable lake, situated at an altitude of 3,809 meters above sea level (m.a.s.l.) [9]. It is a water body between two countries, Peru and Bolivia, and is part of the endorheic basin of the Andean Altiplano. The lake covers an area of approximately 8,560 km2, with a maximum length of about 190 kilometers and a maximum width of around 80 kilometers. Its average depth is 108 meters, with a maximum depth of 282 meters. Lake Titicaca is fed by five primary river systems and several smaller streams [17]. The region experiences a cold, tropical climate, with the lowest temperatures occurring in July, ranging from -1.6°C to 5.1°C, and the highest temperatures in November, reaching between 13.5°C and 16.0°C.

In terms of precipitation, the wettest months typically span from December to March, averaging 195.3 mm, while the driest period is observed between May and August, with precipitation levels as low as 6.13 mm [18]. This lake is home to a wide variety of fauna, including over 100 bird species such as Phalaropus tricolor, Pterocnemia pennata, and the endangered species Rollandia microptera, amphibians like Rhinella spinulosa, Pleurodema marmoratum, Gastrotheca marsupiata, and the critically endangered Telmatobius coleus. The lake also hosts various fish species like Orestias, Trichomycterus, Oncorhynchus mykkis, and Odonthestes bonariensis, as well as some reptiles including Liolaemus, Proctoporus, and Tachymenis peruviana. Additionally, several mammal species are present in the region, such as Oligoryzomis andinus, Cavia tschudii, Lagidium peruanum, and Pseudalopex culpaeus [19], [20]. The flora of Lake Titicaca and its surrounding areas includes 21 species of aquatic and semi-aquatic plants, along with 153 terrestrial species. Among the notable examples are Elodea, Myriophyllum, Zannichellia, and Schoenoplectus tatora, commonly known as "totora." Totora is vital in the local ecosystem and community, being used for food, constructing homes and islands, crafts, and boat-making. This versatile plant covers up to 60% of the Lake Titicaca Natural Reserve [20].

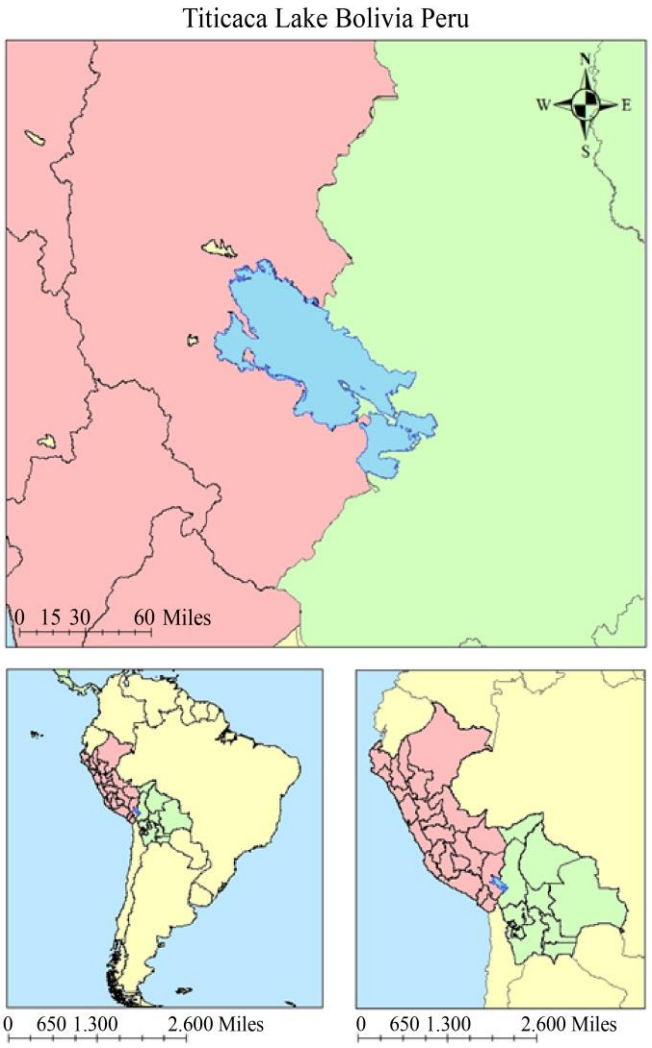

Fig. 1 Selected study area

Given that the lake is situated between two countries, it is relevant to understand the demographics of the surrounding regions. On the Peruvian side, the region of Puno, which encompasses Lake Titicaca, had an estimated population of 1,226,353 in 2022 [21]. On the Bolivian side, the estimated population in 2022 was 3,051,947 [22]. The lake and its surroundings host various economic activities. The aquaculture sector is primarily based on farming rainbow trout (Oncorhynchus mykiss) in small-scale and semi-artisanal fish farms.

This activity is essential as it produces more than 43 tons per year, representing at least 80% of the national production [23], [24]. Additionally, tourism is a significant economic activity as the lake is part of the central Andes tourist circuit, attracting millions of tourists each year, generating benefits for the local population and contributing to maintaining the Lake's Natural Protected Area [25], [26]. On the other hand, mining activities harm the lake, as they are the primary sources of water contamination due to mercury and heavy

metals [27]. It is crucial to highlight that harmful algal blooms (HABs) releasing toxins can severely compromise water quality, making it unsafe for consumption and irrigation. These blooms also negatively impact recreational activities, with significant repercussions on economic sectors such as aquaculture and tourism, both of which can suffer due to the excessive proliferation of algae [28].

3.2. Data Sets

This study used datasets from Landsat 8, a satellite launched on February 11, 2013 [29]. Currently, it is operated by the United States Geological Survey (USGS), which performs calibrations, operations, data generation, and archiving at the Earth Resources Observation and Science (EROS) Center [30]. The satellite is equipped with the Operational Land Imager (OLI) and Thermal Infrared Sensor (TIRS) [31]. Some technical specifications of Landsat 8 are shown in the following table.

The OLI operates in the visible, near-infrared, and short-wave infrared bands, while the TIRS operates in two thermal bands. The characteristics of the spectral bands of OLI and TIRS can be observed in the following table.

Table 1. Technical specifications of Landsat 8 satellite

	Landsat 8
Scenes/Day	~650
Sensor type	Pushbroom (both OLI and TIRS)
Radiometric resolution	12 bits
Temporal resolution	16 days
Orbit	705 Km Sun-Sync 98.2° inclination (WRS2)

Table 2. Spectral Bands of OLI and TIRS

Band	**Name**	**Wavelength (µm)**	**Resolution (m)**
1	Ultra Blue (coastal/aerosol)	0,435 - 0,451	30
2	Blue	0,452 - 0,512	30
3	Green	0,533 - 0,590	30
4	Red	0,636 - 0673	30
5	Near Infrared (NIR)	0,851 - 0,879	30
6	Shortwave Infrared 1 (SWIR 1)	1,566 - 1,651	30
7	Shortwave Infrared 2 (SWIR 2)	2,107 - 2,294	30
8	Panchromatic	0,503 - 0,676	15
9	Cirrus	1,363 - 1,384	30
1	Thermal Infrared (TIR 1)	10,60 - 11,19	100
1	Thermal Infrared (TIR 2)	11,50 - 12,51	100

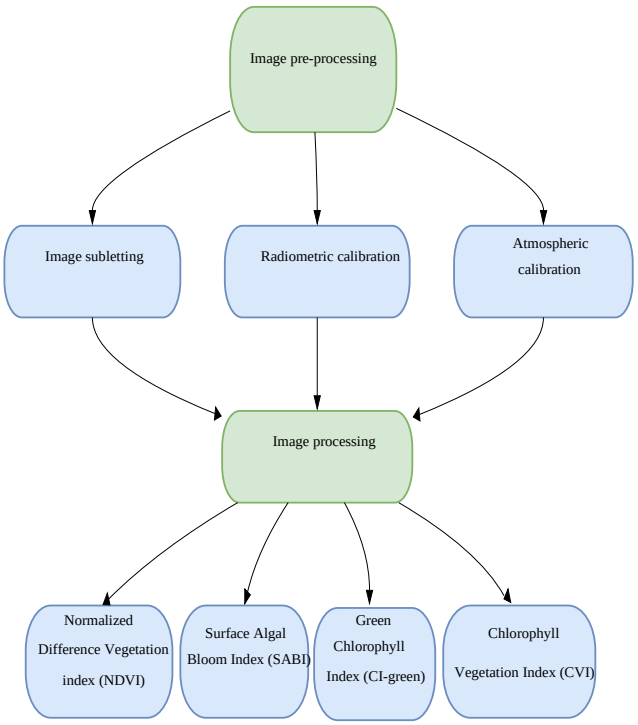

Fig. 2 Block diagram

Landsat 8 is equipped with 11 spectral bands and has a spatial resolution of 15 meters for the panchromatic band, 30 meters for the multispectral bands, and 100 meters for the thermal bands [32]. The selected datasets were filtered based on date criteria, from 01/01/2018 to 09/10/2023. Additionally, the Region of Interest (ROI) criterion was applied using the shapefile of Lake Titicaca. Similarly, the cloud coverage criterion was considered in the scene, selecting only images with a cloud coverage of less than 10%.

3.3. Treatment of Satellite Images

For image treatment, a pre-processing step will be performed in the first stage, as shown in Figure 2. The pre-processing step involves the selection of a subset of images and radiometric and atmospheric calibrations to reduce errors. In order to perform the radiometric calibration process, it is necessary to calculate the Top-of-Atmosphere (TOA) reflectance [33], for which the following equation must be applied:

$$\rho = \frac{\pi L_\lambda d^2}{ESUN_\lambda \sin\theta} \quad (1)$$

Where:

L_λ = TOA spectral radiance ((Watts/(m²*srad*µm))

d = earth-sun distance, in astronomical units

$ESUN_\lambda$ = solar irradiance (Watts/(m²*µm))

Θ = sun elevation in degrees

As can be seen in equation (1), it is necessary to have the TOA spectral radiance [34], for which we must apply the following equation:

$$L_\lambda = Gain * pixel * offset \quad (2)$$

Where:

L_λ= TOA spectral radiance ((Watts/(m²*srad*µm))

Gain (Watts/(m²*srad*µm))

Offset (Watts/(m²*srad*µm))

In the next step, which is the processing stage, we must find the indices that allow us to study the presence of algae in Lake Titicaca. The Normalized Difference Vegetation Index (NDVI) is one of the most widely used vegetation indices due to its high sensitivity to vegetation variations, as it leverages the property of plants to reflect the visible and near-infrared spectrum [35]. It is based on a relationship between reflectance in the Near-Infrared Spectrum (NIR) and red and is calculated as follows:

$$NDVID = \frac{NIR-Red}{NIR+Red} \quad (3)$$

The Green Chlorophyll Index (CI-Green) is sensitive to changes in leaf chlorophyll content [36]. It is calculated using the following formula:

$$CI_{green} = \frac{NIR}{Green} - 1 \quad (4)$$

On the other hand, the Surface Algal Bloom Index (SABI) is used to detect biomass on water surfaces, as it considers spectral bands sensitive to bodies of water [37], [38] and is calculated as follows:

$$SABI = \frac{NIR-Red}{Blue+Green} \quad (5)$$

Finally, the Chlorophyll Vegetation Index (CVI) is an index sensitive to chlorophyll content in leaves and insensitive to variations in leaf area [39]. It incorporates reflectances in the NIR, red, and green spectra, and its formula is:

$$CVI = \frac{NIR}{Green} * \frac{Red}{Green} \quad (6)$$

4. Results and Discussion

The data obtained from Landsat 8 spans from January 1, 2018, to October 9, 2023, separated into six parts corresponding to the yearly averages of each index, resulting in 6 images for each index (NDVI, CI-Green, SABI, and CVI). These indices were calculated using the Google Earth Engine platform.

The processed images were used to create thematic maps, one for each index, and each map is divided into six parts, each corresponding to a year within the 2018-2023 period. Additionally, the range values for each index are displayed, and each is detailed below.

4.1. Normalized Difference Vegetation Index (NDVI)

The maps with the results of the NDVI calculation are shown in Figure 3. The value range goes from -1 to 1, where the minimum values represented in orange are related to the absence of vegetation or dead vegetation; values between 0 and ~0.2 indicate, in this context, land and materials dissolved in the lake represented in yellow. The other values indicate the presence of some type of vegetation, becoming more intense (green shades) with increasing vitality.

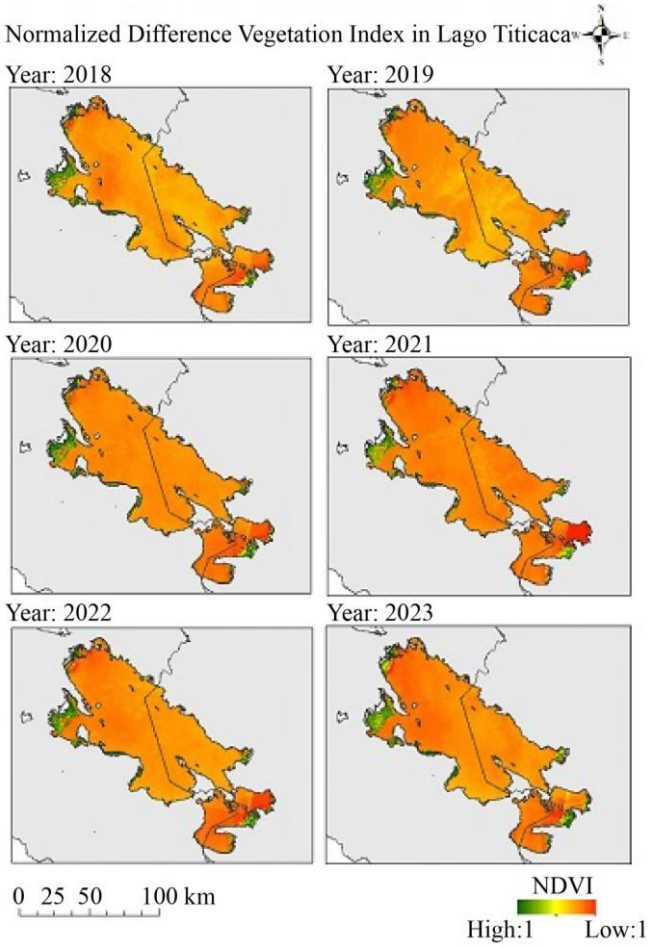

Fig. 3 Normalized difference vegetation index map

In addition, the calculated statistical raster data is shown in Table 3, with the highest average being -0.227804 for 2022, while the lowest average obtained was -0.306569 for 2021.

Table 3. Statistics of the NDVI

	Statistics (NDVI)			
Year	**Min**	**Max**	**Mean**	**Std Dev.**
2018	-0.824869	0.638841	-0.288712	0.164989
2019	-0.835117	0.624375	-0.285024	0.160860
2020	-0.782668	0.622725	-0.271408	0.164667
2021	-0.799485	0.661264	-0.306569	0.171245
2022	-0.772973	0.628409	-0.227804	0.154315
2023	-0.702427	0.593869	-0.278702	0.151622

4.2. Chlorophyll Index Green (CI-Green)

In the case of the CI-Green, the maps created are displayed in Figure 4. Its value ranges from -1 to 4, where values between -1 and 1 (depicted in violet-blue tones) signify the absence of vegetation in those areas. As the values progressively increase (shifting from yellow to green), it indicates the presence of plants, with the particularity that this index better reflects the canopy of the algae community.

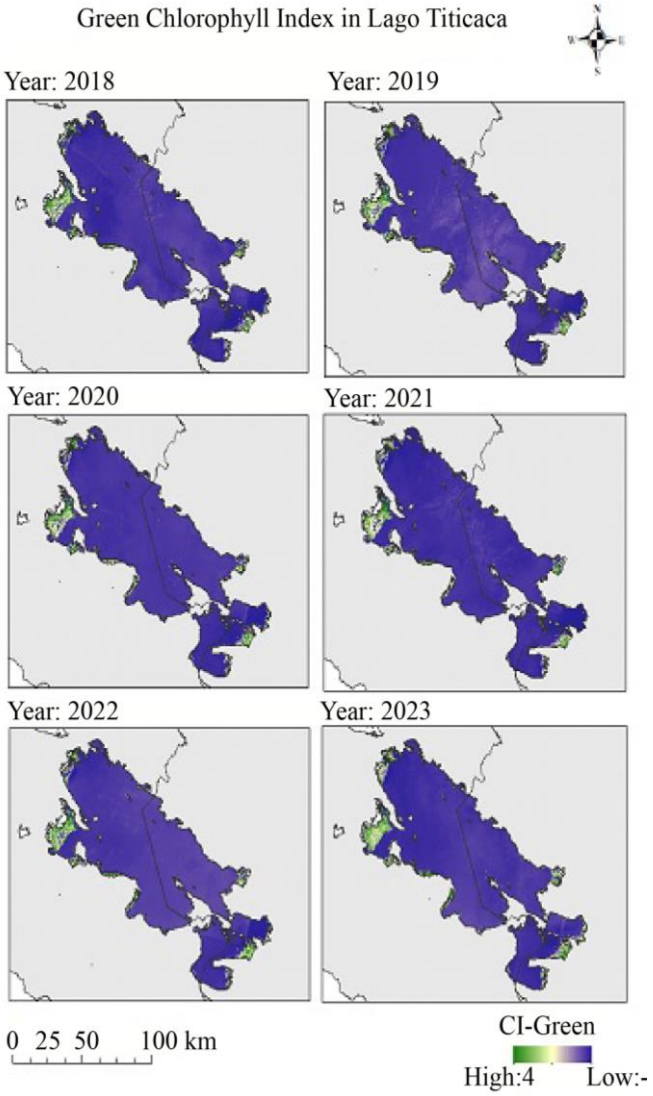

Fig. 4 Green chlorophyll index map

Furthermore, the calculated statistical data for these rasters are presented in Table 4, where it can be noted that the maximum average value is -0.497915, corresponding to the year 2022. On the other hand, the minimum value is -0.592198, which was obtained for the year 2021.

4.3. Surface Algal Bloom Index (SABI)

For the SABI, the maps are displayed in Figure 5. This index's values are within the range of -1 to 2, where the most negative values represent the presence of water, indicated by a bluish tone. Values between 0 and 1 signify a low presence of surface algae with greenish colors. Values above 1 indicate a high algae bloom on the water's surface, depicted in reddish tones on the maps.

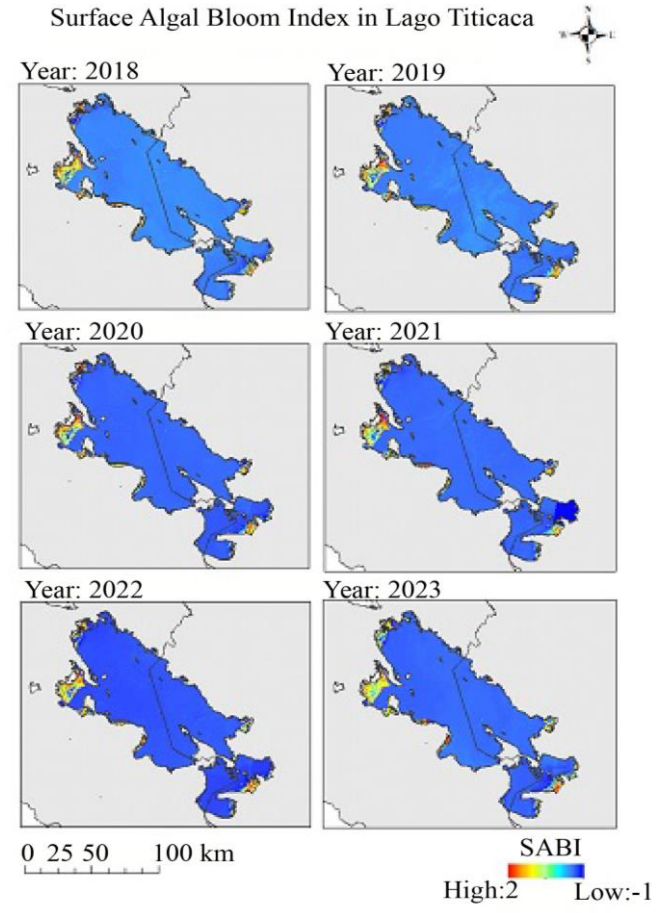

Fig. 5 Surface algal bloom index map

Table 4. Statistics of the CI-Green

	Statistics (CI-Green)			
Year	**Min**	**Max**	**Mean**	**Std Dev.**
2018	-0.934856	3.387172	-0.574179	0.418901
2019	-0.940751	3.177682	-0.568350	0.404831
2020	-0.914493	3.519428	-0.539640	0.445323
2021	-0.915721	3.620948	-0.592198	0.443533
2022	-0.923395	3.044029	-0.497915	0.425578
2023	-0.874902	3.012194	-0.562090	0.408698

Table 5. Statistics of the SABI

	Statistics (SABI)			
Year	**Min**	**Max**	**Mean**	**Std Dev.**
2018	-0,533692	1,712797	-0,067743	0,142638
2019	-0,536530	1,471269	-0,070682	0,133664
2020	-0,482980	1,666416	-0,059143	0,154990
2021	-0,491686	1,923333	-0,067671	0,152715
2022	-0,420455	1,475345	-0,054545	0,149326
2023	-0,355696	1,455210	-0,068741	0,124002

Statistical data for the raster images presented in Table 5 shows the following trends: The minimum values ranged from -0.536530 in 2019 to -0.355696 in 2023, while the maximum values varied between 1.455210 in 2023 and 1.923333 in 2021. The mean values were relatively stable, ranging from -0.070682 in 2019 to -0.054545 in 2022. Standard deviations showed slight variations, with the highest being 0.154990 in 2020 and the lowest 0.124002 in 2023. These figures highlight consistency across the years, with minor fluctuations.

4.4. Chlorophyll Vegetation Index (CVI)

Finally, the maps containing the representation of CVI are shown in Figure 6. The range in which the values for this index vary is from 0 to 5, where values below 2.5 represent areas without chlorophyll, in this case, the lake water corresponding to the color blue. On the contrary, values between 2.5 and 5 indicate areas with chlorophyll activity, with higher activity approaching 5. Regarding color, as values approach 5, the areas become greener.

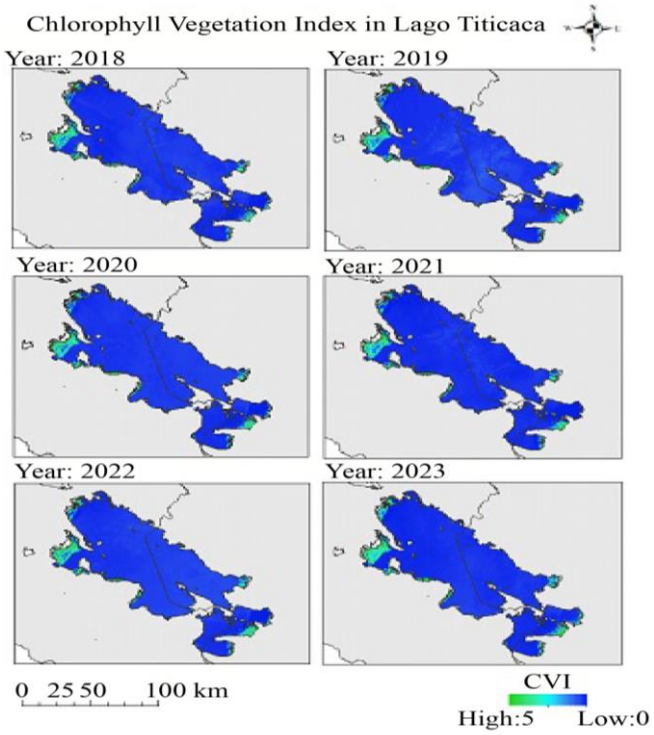

Fig. 6 Chlorophyll vegetation index map

Table 6. Statistics of the CVI

	Statistics (CVI)			
Year	**Min**	**Max**	**Mean**	**Std Dev.**
2018	0,041668	4,205159	0,318386	0,460238
2019	0,039133	4,208795	0,329534	0,453644
2020	0,059972	4,881822	0,351812	0,473648
2021	0,036473	4,346753	0,302341	0,471120
2022	0,045829	4,333558	0,388543	0,469201
2023	0,045728	4,897398	0,347167	0,516264

Like in previous cases, the calculated statistical data in Table 6 shows a maximum mean of 0.388543 in 2022 and a minimum mean of 0.302341 in 2021. Minimum values ranged from 0.036473 (2021) to 0.059972 (2020), while maximum values varied from 4.205159 (2018) to 4.897398 (2023).

4.5. Areas Covered by Algae

Considering the values from which algae is recorded in each index, a table (Table 7) was prepared showing the results of calculating areas (in km2) with these characteristics, ordered according to the years of study. The different indices used locate concentrations of vegetation (algae) and chlorophyll activity in the same areas, which correspond to some provinces in Puno, such as Huancané, Puno, El Collao, and Chucuito, as well as in La Paz, including Omasuyos, Los Andes, and Ingavi. The color coding in the visualization illustrates the proliferation of Harmful Algal Blooms (HABs), highlighting their spread to new areas over time. On the other hand, the color intensity reflects an increase in algae concentration for the year 2023 in areas where they were already present since 2018.

From the statistical data presented in Tables 3-6, when sorted from highest to lowest according to the mean values, all indices agree that the highest averages correspond to 2022, followed by 2020. For the remaining years, all indices align except for SABI. This discrepancy might be due to the cycle of seasonal temperatures, as algae tend to bloom less in colder temperatures and, therefore, might not have a significant presence on the surface [40]. However, from the maps, we can see that SABI does detect the annual increase in the area occupied by algae, just like the other indices. From Table 7, we can see that the areas covered with algae, although fluctuating as the years go by, also show a tendency to grow, reaching their maximum expansion in 2023 for all indices, making the lake's situation increasingly concerning. As can be observed in Table 7, the year 2023 is the year that shows the highest vegetation coverage, according to the NDVI index, within the lake's water body, with an area of 604.2 km^2. On the other hand, concerning the CI-Green index, it has the largest area of chlorophyll presence within the lake's water body in 2023, covering a total surface of 515.4 km^2. Additionally, regarding the CVI index, in the year 2023, it exhibits the largest chlorophyll presence within the lake's water body, covering an area of 510.1 km^2.

Table 7. Areas covered with algae in Lake Titicaca

	Area with the presence of algae detected by each index (km^2)			
Year	**NDVI**	**CI-green**	**SABI**	**CVI**
2018	529.6	453.6	482.4	423.6
2019	539.0	439.6	472.1	405.5
2020	548.8	471.3	501.1	435.4
2021	514.3	442.5	473.0	409.1
2022	514.3	481.4	473.0	446.7
2023	604.2	515.4	531.9	510.1

Table 8. Comparison between this study and others

Study	Place	Years	Used indexes
Kiage & Walker [2]	Lake Maracaibo, Venezuela	2003-2006	NDVI
Perreira et al. [9]	Lake Titicaca, Peru-Bolivia	2013	Ocean Color Algorithms (OC3, OC2443, OC2483)
Malahlela et al. [15]	Vaal Dam, South Africa	2014-2015	Difference Vegetation Index (DVI)
Guachalla et. al. [16]	San Roque Reservoir, Argentina	2017	Trophic State Index (TSI)
This study	Lake Titicaca, Peru-Bolivia	2018-2023	NDVI, CI-Green, SABI, CVI

Finally, concerning the SABI index, which provides information about the surface with algal blooms, 2023 has the highest algal blooms, totaling 531.9 km^2. The mentioned areas that indicate experiencing algae blooms in Lake Titicaca, according to the observed analysis of the four indices, cover a significant area, equivalent to a range of 5.95% to 7.05% of the total area of Titicaca Lake. Table 8 displays some characteristics of studies like this one that focus on identifying chlorophyll concentrations in water bodies. Similarly to [2], the NDVI index, spanning several years, was applied. NDVI findings reveal that algae proliferation in parts of Lake Titicaca stems from pollution by local populations and industries. Notably, [2] employed images from specific dates to identify peak algal growth seasons. Conversely, our annual averages approach offers a clearer view of how algae's presence has evolved over time. In both the study [9] and the current investigation, Lake Titicaca has been the focal point of our research. Study [9] emphasizes the validation of algorithms through simulations, presenting maps that pinpoint areas with elevated chlorophyll-a concentrations, a marker for the presence of algae and active chlorophyll processes. This parallels our study's findings, where we deploy advanced mapping techniques to delineate lake zones exhibiting significant algae presence and chlorophyll activity. Our work extends beyond the foundational analysis presented in [9], incorporating a broader dataset and applying enhanced algorithmic approaches to refine the accuracy of identifying chlorophyll-rich areas, thereby contributing to a more comprehensive understanding of the ecological dynamics of Lake Titicaca.

The harmful algal blooms detected in Lake Titicaca between 2018 and 2023 show a worrying trend of expansion, reaching their peak in 2023, with affected areas ranging from 510.1 km^2 to 604.2 km^2 based on the indices (NDVI, CI-Green, SABI, CVI). A similar pattern can be observed when compared to Lake Okeechobee, where harmful algal blooms impacted 70% of its surface. In both cases, the proliferation of these blooms has been closely linked to increased anthropogenic activities such as urbanization, agriculture, and wastewater discharge, which elevate nutrient levels in water bodies. The satellite data utilized in this study and historical records trace algae growth tied to the lake's ongoing eutrophication, particularly in areas with high human activity. The effectiveness of employing single and double bands for chlorophyll-a detection was evaluated, concluding that indices utilizing two or more bands yield superior outcomes. This enhanced accuracy is primarily due to the interaction between bands, allowing for correcting reflectance errors. This research employed the CI-Green and CVI indices, specifically designed to increase sensitivity to chlorophyll presence by integrating reflectance in the green band. This approach corroborates the findings in [15], emphasizing the improved detection capabilities using multi-band indices. About [16], the Trophic State Index (TSI) was employed to assess its effectiveness in identifying chlorophyll-a concentrations. A map delineating different classes based on index values was showcased to facilitate this evaluation, mirroring the SABI maps utilized in this research. Such a mapping approach proves invaluable when the goal is to graphically represent the intensity of specific attributes through color coding, offering a visual means to discern the distribution and concentration of chlorophyll-a within a water body.

5. Conclusion

Lake Titicaca, a vital binational water body, supports diverse species of flora and fauna while serving as a key driver of economic and tourism activities. Given its ecological and economic significance, ensuring its proper conservation is paramount. As observed, Earth observation satellites are crucial tools that allow us to collect information about a study area without direct contact. In this case, the Landsat 8 satellite mission was utilized to calculate various indices to highlight the presence of Harmful Algal Blooms. This analysis was conducted from January 2018 to October 2023, and four indices were calculated, including the Normalized Difference Vegetation Index (NDVI), Green Chlorophyll Index (CI-Green), Surface Algal Bloom Index (SABI), and Chlorophyll Vegetation Index (CVI). Thematic maps for each index were also developed, revealing that since 2018, certain regions have shown significant concentrations of vegetation (algae) and chlorophyll activity. In Peru, these areas are concentrated in Huancané, Puno, El Collao, and Chucuito provinces. In Bolivia, similar patterns of algal presence and photosynthetic activity were detected in the provinces of Omasuyos, Los Andes, and Ingavi. The analysis indicates that areas of Lake Titicaca affected by algal blooms cover a significant range, from 510.1 km^2 to 604.2 km^2 at the maximum index values, representing 5.95% to 7.05% of the lake's total area. The insights from this research offer substantial value to local policymakers and environmental managers in both nations, providing a data-driven basis for resource allocation and targeted remediation strategies. By pinpointing areas with persistent chlorophyll activity from 2018 to 2023, these maps

enable authorities to prioritize and streamline cleaning and conservation efforts effectively. Furthermore, understanding these algal blooms' spatial distribution and temporal evolution can inform future environmental planning and policy development, fostering more sustainable management of aquatic ecosystems. This strategic approach not only aims to mitigate the immediate impacts of Harmful Algal Blooms (HABs) but also contributes to the long-term health and resilience of affected water bodies, benefiting the environment and local communities.

References

[1] Jiabin Yu et al., "Water Eutrophication Evaluation Based on Multidimensional Trapezoidal Cloud Model," *Soft Computing*, vol. 25, pp. 2851-2861, 2021. [CrossRef] [Google Scholar] [Publisher Link]

[2] Lawrence M. Kiage, and Nan D. Walker, "Using NDVI from MODIS to Monitor Duckweed Bloom in Lake Maracaibo, Venezuela," *Water Resources Management*, vol. 23, pp. 1125-1135, 2009. [CrossRef] [Google Scholar] [Publisher Link]

[3] S. Warner et al., Acknowledgements United Nations Environment Programme Global Environment Monitoring System for Freshwater (UNEP GEMS/Water), 2021. [Online]. Available: www.sdg6monitoring.org

[4] Uroosa et al., "Insights into the Effects of Harmful Algal Bloom on Ecological Quality Status Using Body-Size Spectrum of Biofilm-Dwelling Ciliates in Marine Ecosystems," *Marine Pollution Bulletin*, vol. 160, 2020. [CrossRef] [Google Scholar] [Publisher Link]

[5] Florida Department of Environmental Pretection, "Blue-Green Algal Bloom Weekly Update," 2023. [Online]. Available: https://floridadep.gov/sec/sec/documents/blue-green-algal-bloom-weekly-update-december-7-2023

[6] G. Free et al., "An EU Analysis of the Ecological Disaster in the Oder River of 2022," *Publications Office of the European Union*, 2023. [CrossRef] [Google Scholar] [Publisher Link]

[7] German Augusto Murrieta-Morey et al., "Black-Banded Fish Myloplus Schomburgkii Mortality Due to Poor Water Quality Associated with Dickweed Overpopulation in a Breeding Pond in the Peruvian Amazon," *Folia Amazonica*, vol. 30, no. 1, pp. 107-112, 2021. [CrossRef] [Google Scholar] [Publisher Link]

[8] Liz Romero et al., "Harmful Algal Bloom of the Dinoflagellate Blixaea Quinquecornis in Peru," *Peruvian Magazine of Biology*, vol. 29, no. 1, 2022. [CrossRef] [Google Scholar] [Publisher Link]

[9] Marcela A Pereira-Sandoval et al., "Adjustment of the MODIS OC2 and OC3 algorithms to Obtain the Chlorophyll-a Concentration in Oligotrophic Lakes with Landsat-8: Validation in Lake Titicaca," *Logo Francisco José de Caldas District University*, vol. 7, no. 1, pp. 45-51, 2016. [Google Scholar] [Publisher Link]

[10] Analy Baltodano et al., "Land Cover Change and Water Quality: How Remote Sensing Can Help Understand Driver-Impact Relations in the Lake Titicaca Basin," *Water*, vol. 14, no. 7, pp. 1-19, 2022. [CrossRef] [Google Scholar] [Publisher Link]

[11] Franz Zirena Vilca, "Occurrence of Residues of Veterinary Antibiotics in Water, Sediment and Trout Tissue (Oncorhynchus Mykiss) In the Southern Area of Lake Titicaca, Peru," *Journal of Great Lakes Research*, vol. 47, no. 4, pp. 1219-1227, 2021. [CrossRef] [Google Scholar] [Publisher Link]

[12] Observatorio Binacional del Lago Titicaca, "Evolution of Biophysical Water Quality Parameters From 06/27/19 to 05/01/22 (34 Months) At the Hydromet Buoy Site At 1m Depth, Binational Observatory of Lake Titicaca, 2019. [Online]. Available: https://olt.geovisorumsa.com/boya/DatosMiBoya.html

[13] Jennifer L. Wolny et al., "Current and Future Remote Sensing of Harmful Algal Blooms in the Chesapeake Bay to Support the Shellfish Industry," *Frontiers in Marine Science*, vol. 7, pp. 1-16, 2020. [CrossRef] [Google Scholar] [Publisher Link]

[14] Jisang Lim, and Minha Choi, "Assessment of Water Quality Based on Landsat 8 Operational Land Imager Associated with Human Activities in Korea," *Environmental Monitoring and Assessment*, vol. 187, 2015. [CrossRef] [Google Scholar] [Publisher Link]

[15] Oupa E. Malahlela et al., "Mapping Chlorophyll-a Concentrations in a Cyanobacteria- and Algae-Impacted Vaal Dam Using Landsat 8 OLI Data," *South African Journal of Science*, vol. 114, pp. 9-10, 2018. [CrossRef] [Google Scholar] [Publisher Link]

[16] Andrea Guachalla Alarcón et al., "Spatial Algal Bloom Characterization by Landsat 8-OLI and Field Data Analysis," *IGARSS 2018 - 2018 IEEE International Geoscience and Remote Sensing Symposium*, Valencia, Spain, pp. 929-9295, 2018. [CrossRef] [Google Scholar] [Publisher Link]

[17] Quoc Bao Pham et al., "Prediction of Lake Water-Level Fluctuations Using Adaptive Neuro-Fuzzy Inference System Hybridized with Metaheuristic Optimization Algorithms," *Applied Water Science*, vol. 13, 2023. [CrossRef] [Google Scholar] [Publisher Link]

[18] Jaime Aguilar-Lome, Renato Soca-Flores, and Diego Gómez, "Evaluation of the Lake Titicaca's Surface Water Temperature Using LST MODIS Time Series (2000–2020)," *Journal of South American Earth Sciences*, vol. 112, 2021. [CrossRef] [Google Scholar] [Publisher Link]

[19] Prieto Veramendi, and Patricia Mahela, "Factors Affecting Algal Blooms in High Altitude Lakes at Low Latitude. A Review and the Case of Puno Bay (Lake Titicaca, Peru)," *LA Referencia*, 2021. [Google Scholar] [Publisher Link]

[20] National Service of Protected Natural Areas (SERNANP), PRESIDENTIAL RESOLUTION N° 038 -2021-SERNANP. Peru, 2021. [Online]. Available: https://cdn.www.gob.pe/uploads/document/file/1663413/RP%20N%20038-2021-SERNANP%20-%20COMPLETO.pdf.pdf?v=1612915727

[21] National Institute of Statistics and Informatics (INEI), Puno Statistical Compendium, 2022. [Online]. Available: www.inei.gob.pe
[22] National Statistics Institute, Population and Vital Facts, 2023. [Online]. Available: https://www.ine.gob.bo/index.php/censos-y-proyecciones-de-poblacion-sociales/
[23] Ismena Apaza Quispe, and María del Pilar Blanco Espezua, "Income, Technology and Training of Rural Producers of Trout (Oncorhynchus Mykiss), A Case Study in Lake Titicaca," *Agricultural Science and Technology*, vol. 23, no. 3, 2022. [CrossRef] [Google Scholar] [Publisher Link]
[24] Estefanía Muñoz-Atienza et al., "Local Regulation of Immune Genes in Rainbow Trout (Oncorhynchus Mykiss) Naturally Infected with Flavobacterium Psychrophilum," *Fish & Shellfish Immunology*, vol. 86, pp. 25-34, 2019. [CrossRef] [Google Scholar] [Publisher Link]
[25] Jordi Gascón, and Kevin S. Mamani, "Community-Based Tourism, Peasant Agriculture and Resilience in The Face of COVID-19 in Peru," *Journal of Agrarian Change*, vol. 22, no. 2, pp. 362-377, 2022. [CrossRef] [Google Scholar] [Publisher Link]
[26] Noemi Empress Cayo-Velasquez, Alejandro Apaza-Tarqui, and Cristobal Rufino Yapuchura-Saico, "Tourism Perception and Development in Natural Areas: The Case of Lake Titicaca," *Valdizana Research*, vol. 13, no. 4, pp. 190-203, 2019. [CrossRef] [Google Scholar] [Publisher Link]
[27] François Duquesne et al., "A Coupled Ecohydrodynamic Model to Predict Algal Blooms in Lake Titicaca," *Ecological Modelling*, vol. 440, 2021. [CrossRef] [Google Scholar] [Publisher Link]
[28] Wayne A. Wurtsbaugh, Hans W. Paerl, and Walter K. Dodds, "Nutrients, Eutrophication and Harmful Algal Blooms Along the Freshwater to Marine Continuum," *Wiley Interdisciplinary Reviews: Water*, vol. 6, no. 5, 2019. [CrossRef] [Google Scholar] [Publisher Link]
[29] Landsat Missions, Landsat 8, United States Geological Survey (USGS), 2023. [Online]. Available: https://www.usgs.gov/landsat-missions/landsat-8#science
[30] Landsat Science, LANDSAT 8, 2023. [Online]. Available: https://landsat.gsfc.nasa.gov/satellites/landsat-8/
[31] D. P. Roy et al., "Landsat-8: Science and Product Vision for Terrestrial Global Change Research," *Remote Sensing of Environment*, vol. 145, pp. 154-172, 2014. [CrossRef] [Google Scholar] [Publisher Link]
[32] EOS Data Analytics, Landsat 8 Satellite Images, 2023. [Online]. Available: https://eos.com/find-satellite/landsat-8/
[33] E. Vermote, C. Justice, M. Claverie, and B. Franch, "Preliminary Analysis of The Performance of the Landsat 8/OLI Land Surface Reflectance Product," *Remote Sensing of Environment*, vol. 185, pp. 46-56, 2016. [CrossRef] [Google Scholar] [Publisher Link]
[34] Brian Markham et al., "Landsat-8 Operational Land Imager Radiometric Calibration and Stability," *Remote Sensing*, vol. 6, no. 12, pp. 12275-12308, 2014. [CrossRef] [Google Scholar] [Publisher Link]
[35] Diego Jesús Rodríguez Mauricio, "Temporal Analysis of the NDVI of the Purrumpampa Wetland in Huamachuco and its Relationship with Urban Expansion," *Geographic Magazine of Central America*, vol. 1, no. 70, pp. 429-448, 2022. [CrossRef] [Google Scholar] [Publisher Link]
[36] E. Raymond Hunt et al., "Remote Sensing Leaf Chlorophyll Content Using a Visible Band Index," *Agronomy journal*, vol. 103, no. 4, 2011. [CrossRef] [Google Scholar] [Publisher Link]
[37] Jonah Boucher et al., "Assessing the Effectiveness of Landsat 8 Chlorophyll A Retrieval Algorithm for Regional Freshwater Monitoring," *Ecological Applications*, vol. 28, no. 4, pp. 1044-1054, 2018. [CrossRef] [Google Scholar] [Publisher Link]
[38] Fahad Alawadi, "Detection of Surface Algal Blooms Using the Newly Developed Algorithm Surface Algal Bloom Index (SABI)," *In Proceedings Remote Sensing of the Ocean, Sea Ice, and Large Water Regions 2010, SPIE*, vol. 7825, 2010. [CrossRef] [Google Scholar] [Publisher Link]
[39] M. Vincini, E. Frazzi, and P. D'Alessio, "A Broad-Band Leaf Chlorophyll Vegetation Index at The Canopy Scale," *Precision Agriculture*, pp. 303-319, 2008. [CrossRef] [Google Scholar] [Publisher Link]
[40] Bilbao La Vieja Bracamonte et al., "Spatio-Temporal Analysis of The Expansion of Lemna in the Cohana Bay of the Department of La Paz," Universidad Mayor de San Andrés, 2018. [Google Scholar] [Publisher Link]